DETERMINATION OF A PROVISIONAL STRUCTURAL LAYER COEFFICIENT FOR AN ARAMID SYNTHETIC FIBER MODIFIED ASPHALT MIXTURE

David Timm

Fan Yin

Adam Taylor

March 2, 2021

National Center for Asphalt Technology
NCAT
at AUBURN UNIVERSITY

277 Technology Parkway ■ Auburn, AL 36830

Determination of a Provisional Structural Layer Coefficient for an Aramid Synthetic Fiber Modified Asphalt Mixture

By

Dr. David Timm, P.E.
Brasfield & Gorrie Professor and Associate Chair
Department of Civil and Environmental Engineering
Auburn University

Dr. Fan Yin, P.E.
Assistant Research Professor
National Center for Asphalt Technology
Auburn University, Auburn, Alabama

Adam J. Taylor, P.E.
Assistant Research Engineer
National Center for Asphalt Technology
Auburn University, Auburn, Alabama

March 2, 2021

DISCLAIMER

The contents of this report reflect the views of the authors who are responsible for the facts and accuracy of the data presented herein. The contents do not necessarily reflect the official views or policies of Forta Corporation, the National Center for Asphalt Technology, or Auburn University. This report does not constitute a standard, specification, or regulation. Comments contained in this report related to specific testing equipment and materials should not be considered an endorsement of any commercial product or service; no such endorsement is intended or implied.

ACKNOWLEDGEMENTS

This work was sponsored by Forta Corporation.

INTRODUCTION

Most of the state highway agencies that currently use the '93/'98 AASHTO method for pavement structural design require a layer coefficient of 0.44 for asphalt mixtures, which was originally recommended by the AASHTO Road Test in the 1950's. However, several existing studies have shown that adding aramid synthetic fibers (ASF) can potentially improve the structural capacity of asphalt mixtures due to fiber reinforcement. This improvement may lead to a higher structural coefficient and a reduced asphalt layer thickness, providing significant cost savings for pavement construction. The objective of this study was to determine a structural layer coefficient for an ASF modified asphalt mixture using FORTA-FI®. The study was primarily based on laboratory testing and theoretical structural pavement analysis and design. Two plant-produced mixes were sampled and tested for laboratory performance characterization. The control mixture used a performance graded (PG) 76-22 styrene-butadiene-styrene (SBS) modified binder, while the experimental mixture was produced with ASF in addition to the same PG 76-22 SBS modified binder. Compared to the control mixture, the experimental mixture was evaluated as potential premium mix treatment for providing enhanced structural capacity.

EXPERIMENTAL DESIGN

Mix Design

Table 1 summarizes the volumetrics of the control mix design. The experimental mixture was identical to the control mixture except that ASF was added using a "drop-in" approach during production. The control mix design had a nominal maximum aggregate size (NMAS) of 12.5mm, a PG 76-22 SBS modified binder, and 20% recycled asphalt pavement (RAP). The volumetric optimum binder content (OBC) was 5.0% at an N_{design} of 100 gyrations. Because of a concern that the original mix design lacked adequate cracking resistance, the OBC was increased to 5.4%, which yielded a regressed 3.0% air voids content. The mix design after air voids regression had 14.0% VMA and 79% VFA. Figure 1 presents the Indirect Tensile Asphalt Cracking Test (IDEAL-CT) and Cantabro test results of the mix design at three asphalt binder contents: 5.0%, 5.5%, and 6.0%. At the regressed OBC of 5.4%, the mix design was expected to have adequate durability and intermediate-temperature cracking resistance, as indicated by a predicted IDEAL CT_{index} of 60.0 and a Cantabro mass loss of 6.4% based on linear interpolations.

Table 1. Mix Design and Production QC Volumetrics

Volumetric Properties		Mix Design	Production QC (Control Mix)	Production QC (Experimental Mix)
Aggregate Gradation (Percent Passing)	25mm (1”)	100	100	100
	19mm (3/4”)	100	100	100
	12.5mm (1/2”)	98	99	98
	9.5mm (3/8”)	90	88	87
	4.75mm (#4)	54	52	50
	2.36mm (#8)	40	38	36
	1.18mm (#16)	33	30	29
	0.60mm (#30)	24	21	20
	0.30mm (#50)	13	11	10
	0.15mm (#100)	7	6	6
	0.075mm (#200)	4.1	4.0	3.8
Asphalt Binder Content, %		5.4	5.5	5.3
Dust Proportion		0.9	0.8	0.8
RAP Binder Replacement, %		20	20	21
Rice Gravity (G_{mm})		2.471	2.449	2.456
Bulk Gravity (G_{mb})		2.397	2.400	2.398
Air Voids, %		3.0	2.0	2.4
Aggregate Gravity (G_{sb})		2.637	2.618	2.615
VMA. %		14	13	13
VFA, %		79	85	82

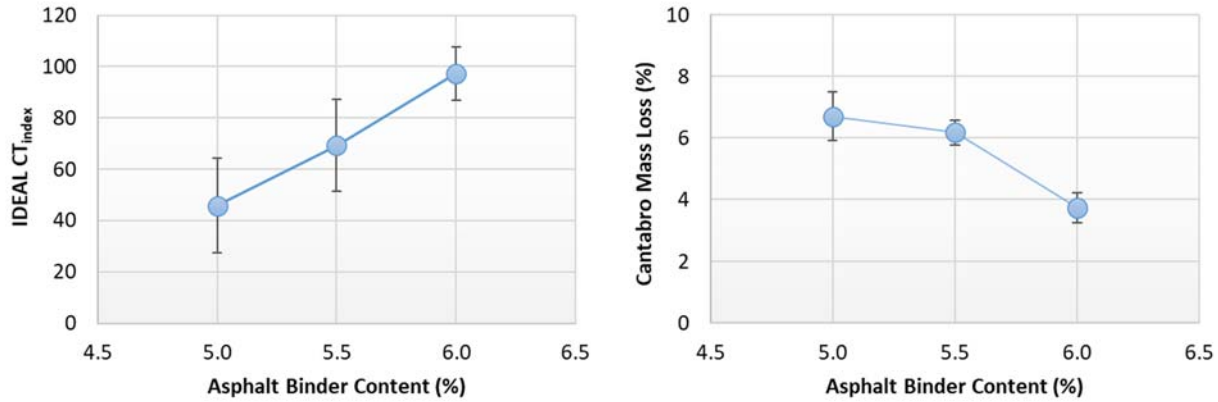

Figure 1. IDEAL-CT and Cantabro Test Results of Control Mix Design at Multiple Asphalt Binder Contents

Mix Production

The control and experimental mixtures were produced at a double-drum asphalt plant in Opelika, Alabama on May 22, 2020. As shown in Figure 2, ASF was added on the RAP conveyor, at a dosage of 1 lbs. per ton of mix, during production of the experimental mixture. Table 1 summarizes the quality control (QC) volumetrics. For both mixes, the differences in asphalt binder content, air

voids, and aggregate gradations between mix design and QC data were within the production tolerance specified in the Alabama Department of Transportation (ALDOT) specification (ALDOT, 2018).

Figure 2. Adding ASF on the RAP Conveyor

Laboratory Tests

During production, the plant mixture was passed through a material transfer vehicle (MTV) and transported to a stockpile sampling location where buckets of mix could be collected. Enough of each plant produced mix was sampled to conduct the Dynamic Modulus (E*) and Bending Beam Fatigue (BBFT) testing in the laboratory. For each test, specimens were fabricated from re-heated plant produced mix that had been reduced to the appropriate testing size per the quartering procedure outlined in AASHTO R47-19. Multiple buckets of each mix were blended in the lab using a quartermaster (AASHTO R47 Mechanical Splitter Type A) to ensure consistency of the plant sample. For both the E* and BBFT tests, specimen air voids were controlled on the final specimen after any required coring and saw trimming.

Dynamic Modulus (E*) specimens were prepared in accordance with AASHTO PP 99-19 *Preparation of Small Cylindrical Performance Test Specimens Using the Superpave Gyratory Compactor (SGC) or Field Cores.* Larger SGC samples were compacted to a diameter of 150 mm and a height of 180 mm prior to four individual test samples being cored from the larger SGC sample. The individual specimens measured 38 mm in diameter and 110 mm in target height after saw trimming. Triplicate specimens per mix were prepared to a target air void level of 7.0 ± 0.5 percent. E* testing was performed in accordance with AASHTO TP 132-19 *Determining the Dynamic Modulus for Asphalt Mixtures Using Small Specimens in the Asphalt Mixture Performance Tester (AMPT).* For a PG 76-22 base binder, this method required the test to be conducted at three temperatures (i.e., 4, 20, and 40°C) and three frequencies (i.e., 10, 1, and 0.1 Hz) for a total of nine unique test conditions. Upon completion of the test and review of data quality, the E* master curve for each mix was constructed in accordance with AASHTO R84-17 *Developing Dynamic Modulus Master Curves for Asphalt Mixtures Using the Asphalt Mixture Performance Tester (AMPT).* Figure 3 shows a photo of a small E* test specimen along with a photo of the Asphalt Mixture Performance Tester (AMPT).

Figure 3. Photo of Small Specimen E* Sample (left) and Photo of AMPT (right)

Bending Beam Fatigue (BBFT) sample fabrication and testing was performed in accordance with AASHTO T321-17 *Determining the Fatigue Life of Compacted Asphalt Mixtures Subjected to Repeated Flexural Bending*. A photo of the BBFT testing apparatus is shown in Figure 4. BBFT specimens were compacted using a rolling wheel compactor and required saw trimming to the appropriate dimensions for testing (380 mm length x 63 mm width x 50 mm height). Nine BBFT specimens were prepared for each mix to a target air void level of 7.0 ± 1.0 percent after saw trimming. BBFT specimens were tested at a temperature of 20°C and a frequency of 10 Hz using a sinusoidal waveform. BBFT testing was performed using a 'fixed reference' device, meaning displacement readings were taken using an LVDT set in a fixed location which referenced a gage point glued to the neutral axis of the beam. The cycles to failure for each individual beam was calculated by determining the cycles to failure corresponding to the peak of the curve developed by multiplying the beam stiffness by the applied cycles (example in Figure 4). Triplicate beam specimens were tested at three different strain levels (i.e., 400, 600, and 800 microstrain) to develop the relationship between applied strain and cycles to failure for each mix.

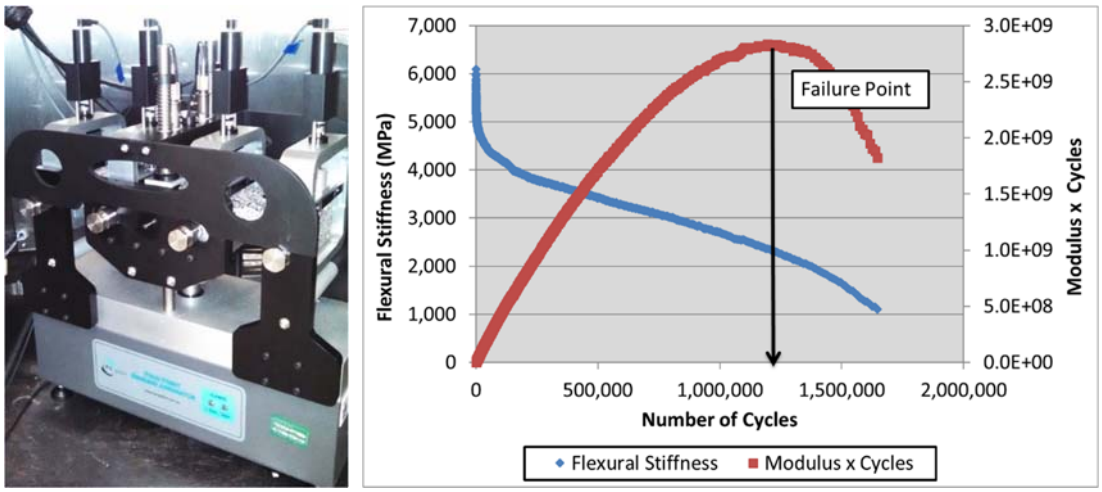

Figure 4. BBFT Test Apparatus (left) and BBFT Cycles to Failure Example (right)

Structural Analysis

The structural analysis focused on estimating the relative difference in expected fatigue cracking performance, and structural coefficients, between the control and experimental mixtures. To that end, the analysis consisted of both layered elastic analysis of theoretical cross-sections in WESLEA for Windows, which produced relative performance expectations and structural coefficients, in addition to estimating the structural coefficient based purely on the measured modulus of each mixture.

Theoretical cross sections were simulated, as depicted in Figure 5, to represent the expected full-scale cross-section that may be built during the summer of 2021 as part of the additive group experiment at the NCAT Test Track. The native Test Track soil and commonly-used aggregate base material, set at 6 inches deep, were used for both cross-sections. The modulus and Poisson ratios were set to representative values based on historical data from Test Track falling weight deflectometer testing and back-calculation. The surface layers were both set to have a Poisson ratio of 0.35 while the modulus values came directly from laboratory testing. Two sets of analyses were conducted. The first used the initial flexural stiffness measured from BBF testing while the second used dynamic modulus measured at 20°C and 10 Hz. The load was simulated as a 20,000 lb single axle with dual tires inflated to 100 psi which represents the 5 trailing single axles on the tractor-triple trailer trucks used at the Test Track. Under these conditions, horizontal tensile strain was computed at the bottom of the asphalt concrete in each section. The tensile strains were then entered into the respective BBF transfer functions from which life estimates were determined.

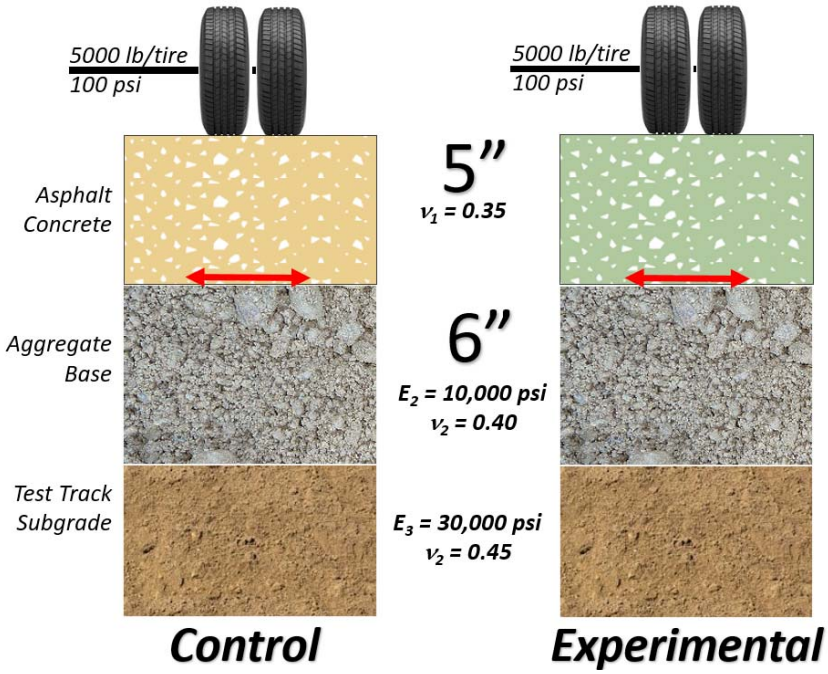

Figure 5. Theoretical Cross-Sections.

The structural analysis described above included quantifying the relative difference in expected fatigue performance lives (i.e., number of cycles to fatigue failure) in addition to estimating an equivalent AC depth to produce the same expected fatigue performance life. The

latter was used to then estimate a structural coefficient of the experimental mixture relative to the control as will be demonstrated in the Structural Analysis Results section discussed below.

The final structural analysis component included estimating structural coefficients based purely on measured modulus values at 20°C, from both flexural stiffness (BBF testing) and dynamic modulus testing, using the empirical correlation chart from the 1993 AASHTO Design Guide (Figure 6). Since the modulus values exceeded the values contained in the chart, a regression equation fit to the chart data was used to extrapolate to the higher measured values in this experiment:

$$a_1 = 0.117 * \ln(E_{AC}) - 1.784 \quad (1)$$

Where:

a_1 = asphalt concrete structural coefficient

E_{AC} = asphalt concrete elastic modulus at 20°C (68°F), psi

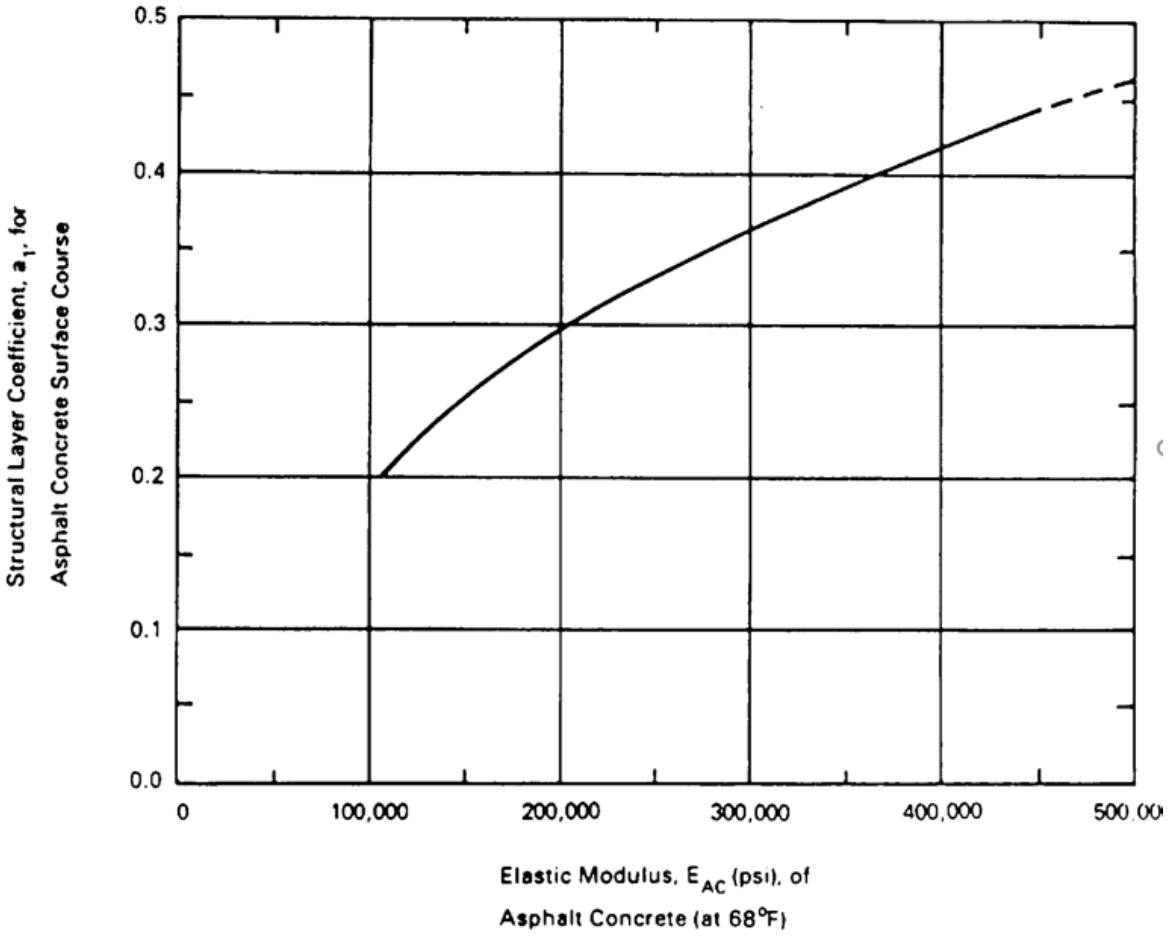

Figure 6. AASHTO a_1 to E_{AC} Correlation (AASHTO, 1993).

LABORATORY TEST RESULTS

Table 2 summarizes the E* and phase angle results of the control versus experimental mixtures. The experimental mixture showed consistently higher E* values than the control mixture, but the differences were marginal (ranged from 3% to 7% only). The two mixes showed almost overlapping E* master curves [Figure 7(a)] at a 20°C reference temperature and a wide range of reduced frequencies. As shown in Figure 7(b), the E* of the experimental mixture was approximately 5.6% higher than that of the control mixture. These results indicated that adding ASF had a slight but insignificant impact on increasing the stiffness of the control mixture. The values measured at 20°C (68°F) and 10 Hz were used in the structural analysis as described above and presented below.

Table 2. Summary of E* Test Results

Temperature (°C)	Frequency (Hz)	Control Mixture		Experimental Mixture	
		E* (psi)	Phase Angle (°)	E* (psi)	Phase Angle (°)
4	10	1,542,041	17.7	1,628,870	17.6
4	1	1,135,936	14.0	1,205,312	14.0
4	0.1	778,466	11.2	830,293	11.1
20	10	728,718	28.2	756,759	28.0
20	1	425,106	24.6	442,849	24.4
20	0.1	223,648	20.2	235,348	20.1
40	10	196,623	25.6	207,452	26.4
40	1	90,165	28.6	95,976	28.8
40	0.1	42,859	29.3	45,208	29.4

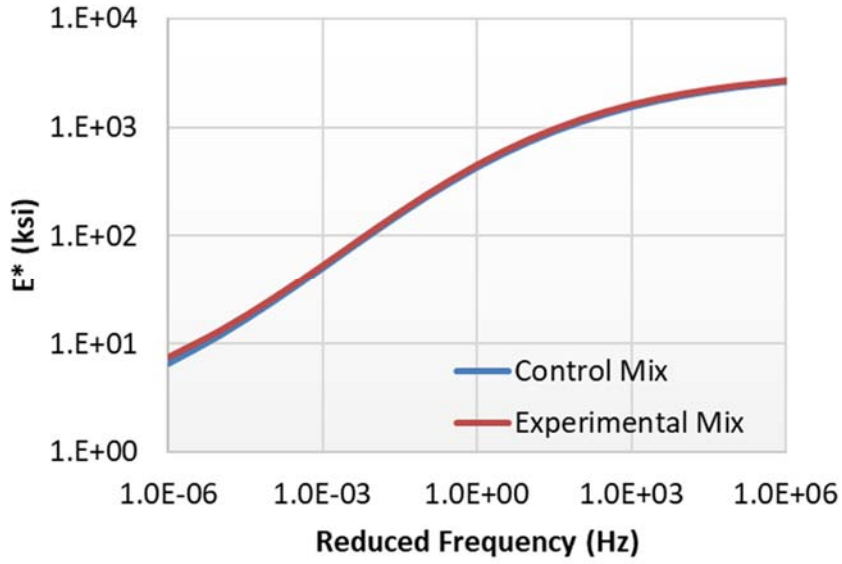

(a)

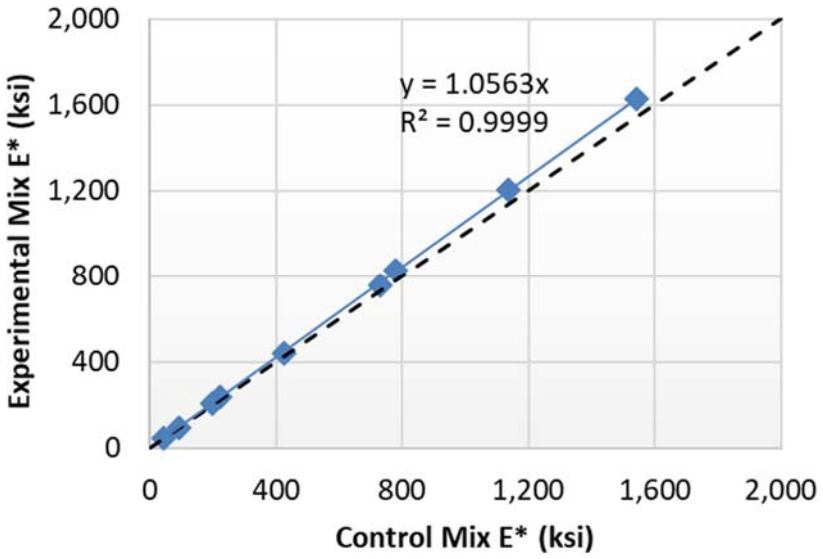

(b)

Figure 7. E* Test Results; (a) 20°C E* Master Curves, (b) Comparison of Control Mixture versus Experimental Mixture

Table 3 summarizes the BBF test results in terms of the average initial beam stiffness and number of cycles to failure (N_f) at three strain levels. In general, the experimental mixture had consistently higher beam stiffness but lower N_f results than the control mixture at 400, 600, and 800 microstrains. These results indicated that adding ASF increased the flexural stiffness but reduced the fatigue resistance of the control mixture at intermediate and high strain levels. Figure 8 presents the N_f versus microstrain plots of the two mixes. Both mixes showed a reasonably strong correlation (R^2 over 0.85) when the results were plotted on a log-log scale. The experimental mixture exhibited a steeper slope than the control mixture, which indicated greater sensitivity of N_f to changes in strain levels in the BBF test. Based on the fitted trendlines in Figure 8, the experimental mixture was expected to outperform the control mixture in terms of fatigue resistance at low strain levels (less than 400 microstrains) as will be discussed more fully in the next section.

Table 3. Summary of BBF Test Results

Mix ID	Microstrain	Replicates	Air Voids (%)	Initial Beam Stiffness (psi)	Cycles to Failure, N_f
Control Mix	400	3	7.2	531,112	2,630,450
	600	3	7.5	497,394	284,725
	800	3	6.5	547,734	64,849
Experimental Mix	400	3	7.8	583,804	2,311,127
	600	3	7.1	605,900	85,112
	800	3	6.7	617,692	11,710

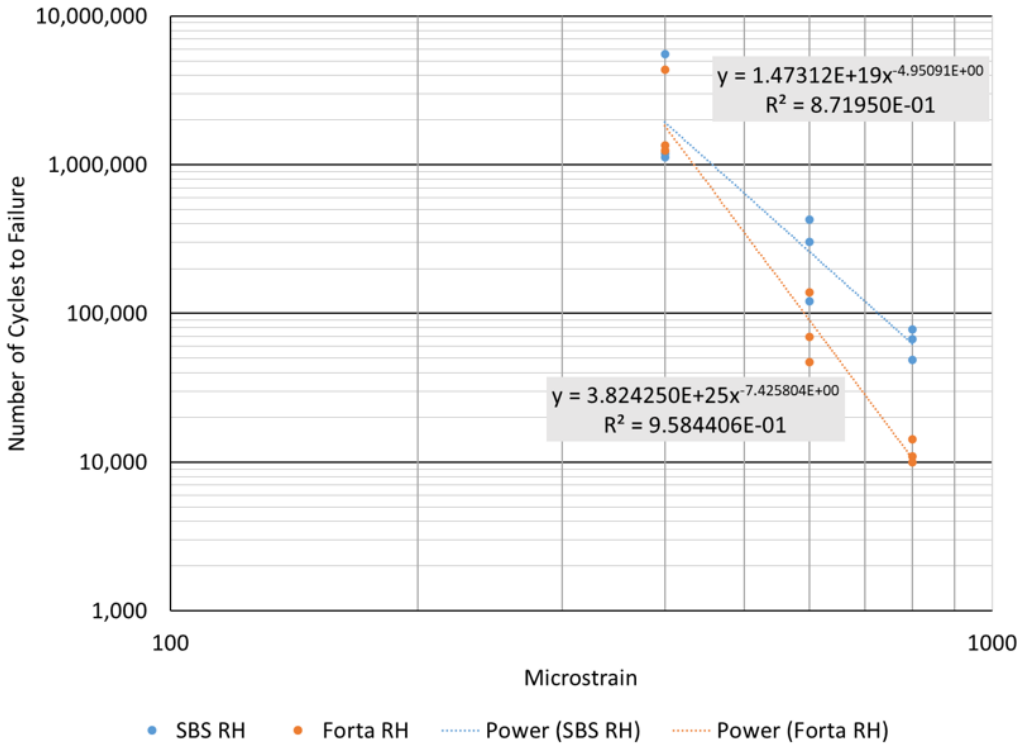

Figure 8. BBF N_f *versus* Microstrain Results

STRUCTURAL ANALYSIS RESULTS

The strain and estimated fatigue life results of using the average flexural beam stiffness, from Table 3, for each asphalt concrete is depicted in Figure 9. As expected, since the experimental mixture has a higher modulus, the resulting strain is lower under the same loading condition. These strain levels were then entered into their respective transfer functions to predict the number of cycles to failure (N), as shown in Figure 9. Rather than focusing on the exact number of cycles predicted, since laboratory beam fatigue data often requires significant shifting to match field conditions, it's important to look at the relative comparison where the experimental mixture is expected to have approximately 5 times the number of loadings to failure under these conditions. This is a function of the reduced strain level and an expectation from extrapolating the respective transfer functions that the experimental mixture will have higher cycles to failure at these low strain values as depicted in Figure 8.

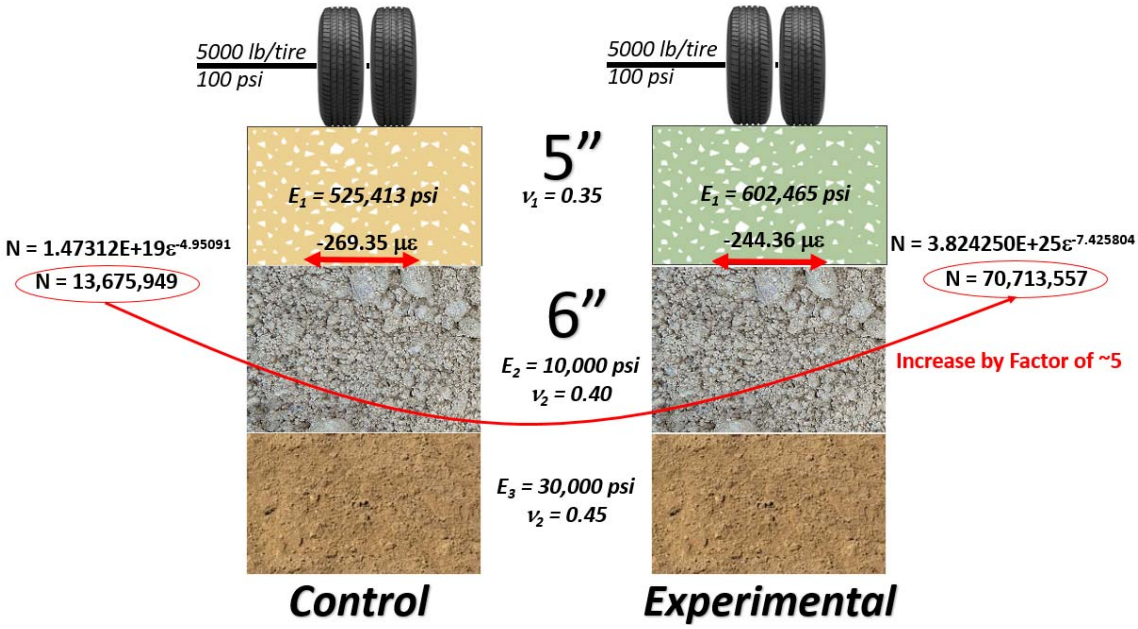

Figure 9. Strain and Fatigue Life Computations Based on AC Flexural Stiffness.

The next part of the analysis determined an experimental AC thickness to produce nearly the same fatigue performance expectation. Using the conditions depicted in Figure 9, it was determined through successive iterations that the experimental AC thickness could be reduced to 4.15 inches, as shown in Figure 10, to achieve nearly the same number of cycles to failure as the control. An exact match between N values was not achieved since it was decided to determine the thickness to the nearest 0.01 inches. This analysis accounts for differences in both the AC moduli and BBF transfer functions.

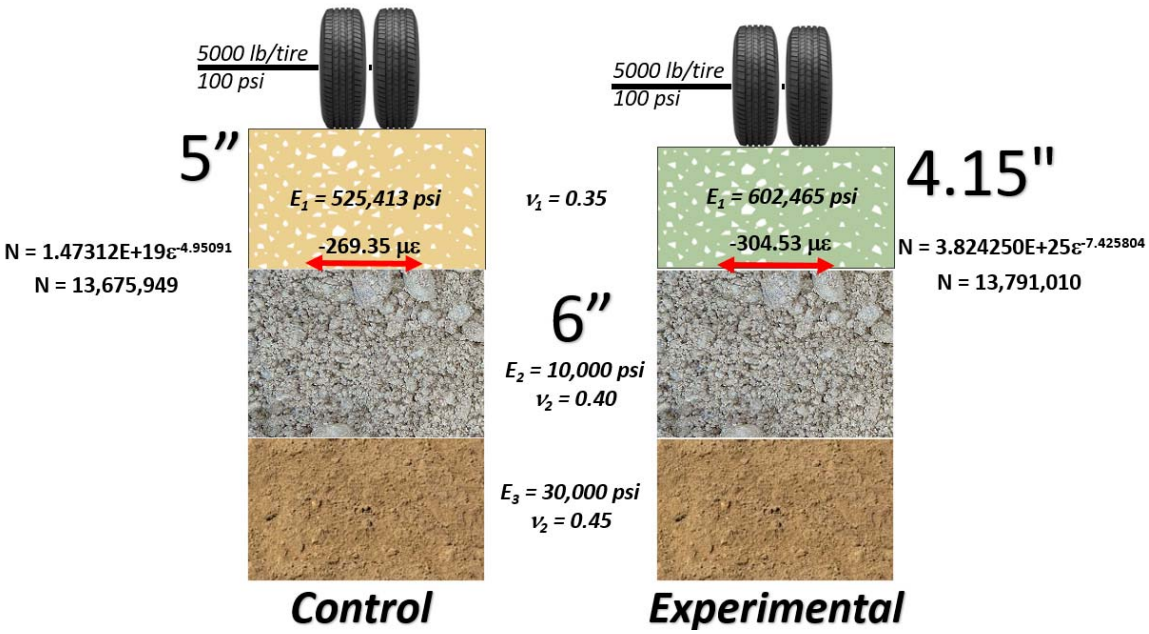

Figure 10. Equivalent Cross Sections Based on Flexural Stiffness.

Once an equivalent thickness was determined a structural coefficient was computed as depicted in Figure 11. For the control section the current structural coefficient for this mix type in Alabama was assigned; 0.54. That value, multiplied by the 5-inch thickness, yielded a structural number of 2.7 for the asphalt concrete layer. Since the structures were considered to be equivalent in terms of fatigue, the 2.7 structural number value was also assigned to the experimental section and the corresponding structural coefficient was computed by dividing the SN by the thickness (4.15 inches) to yield 0.65. This represents a 20% increase over the control.

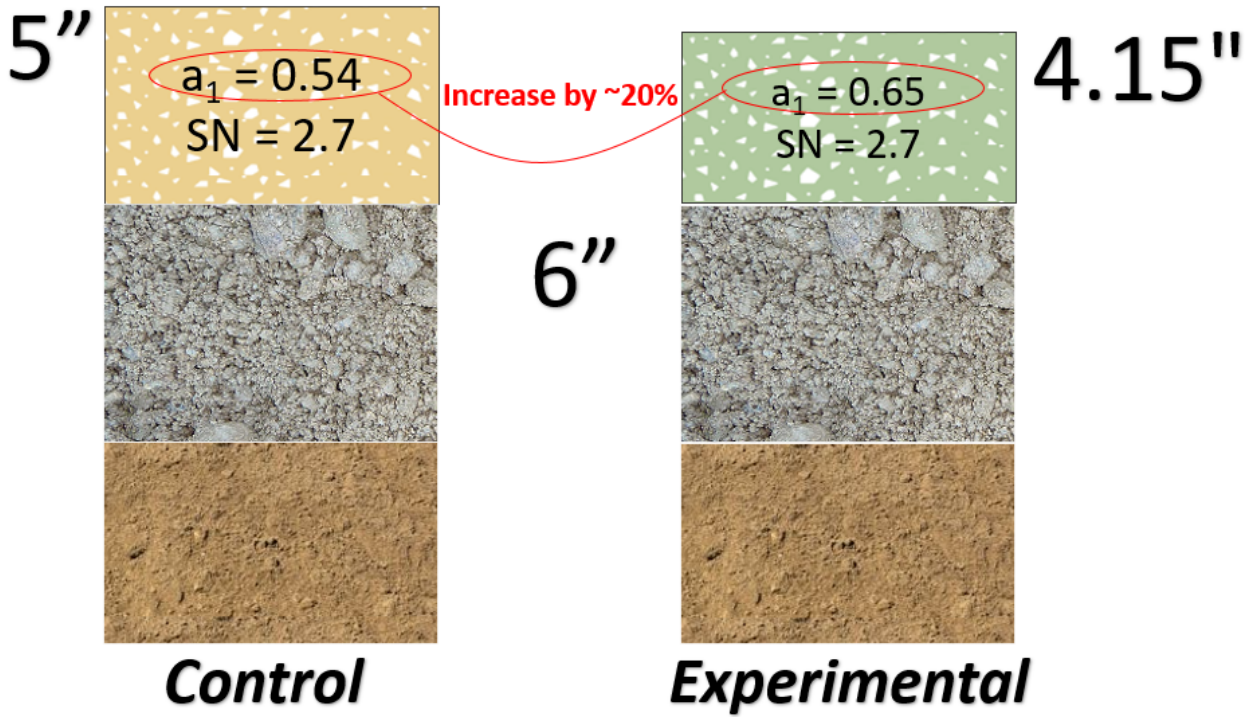

Figure 11. Structural Number Determination Based on Flexural Stiffness.

Following the process described above, the analysis was repeated step-by-step using E* data from Table 2 at 10 Hz and 20°C. Figures 12, 13 and 14 illustrate the relative comparison between the two sections and arrive at very similar conclusions. There was about a six-fold increase in the expected fatigue life for the 5-inch AC thickness and a very similar reduction in the experimental AC thickness compared to the analysis conducted using the flexural AC stiffness. The resulting structural coefficient was also quite similar (0.66 compared to 0.65 in the first analysis). Therefore, regardless of whether flexural stiffness or E* is used in the analysis, the experimental mixture is expected to have better fatigue performance (5 to 6 times better) and a higher structural coefficient (about 20%).

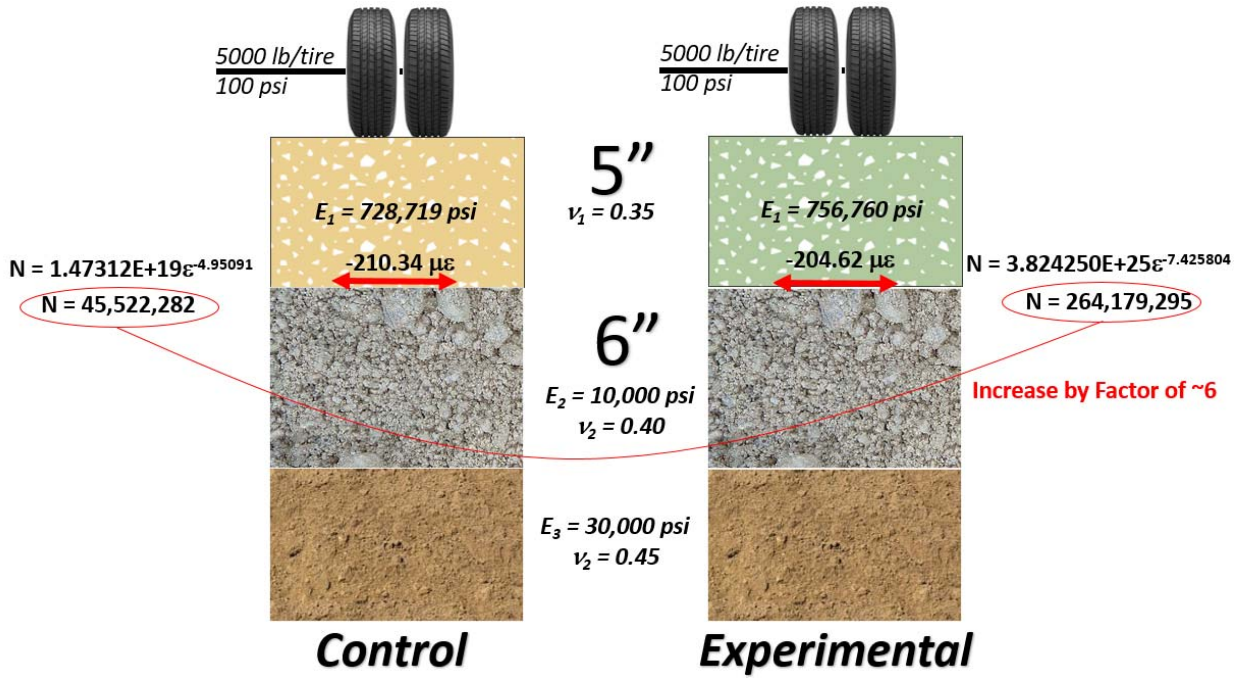

Figure 12. Strain and Fatigue Life Computations Based on E* at 20°C and 10 Hz.

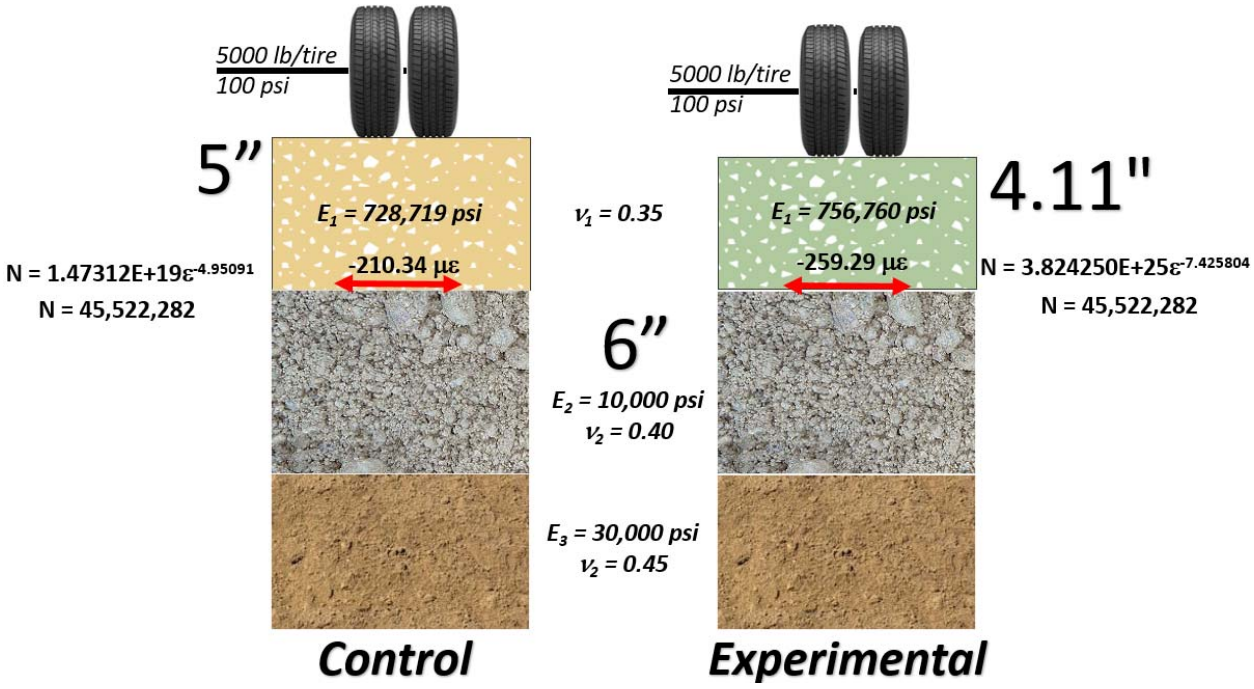

Figure 13. Equivalent Cross Sections Based on E* at 20°C and 10 Hz.

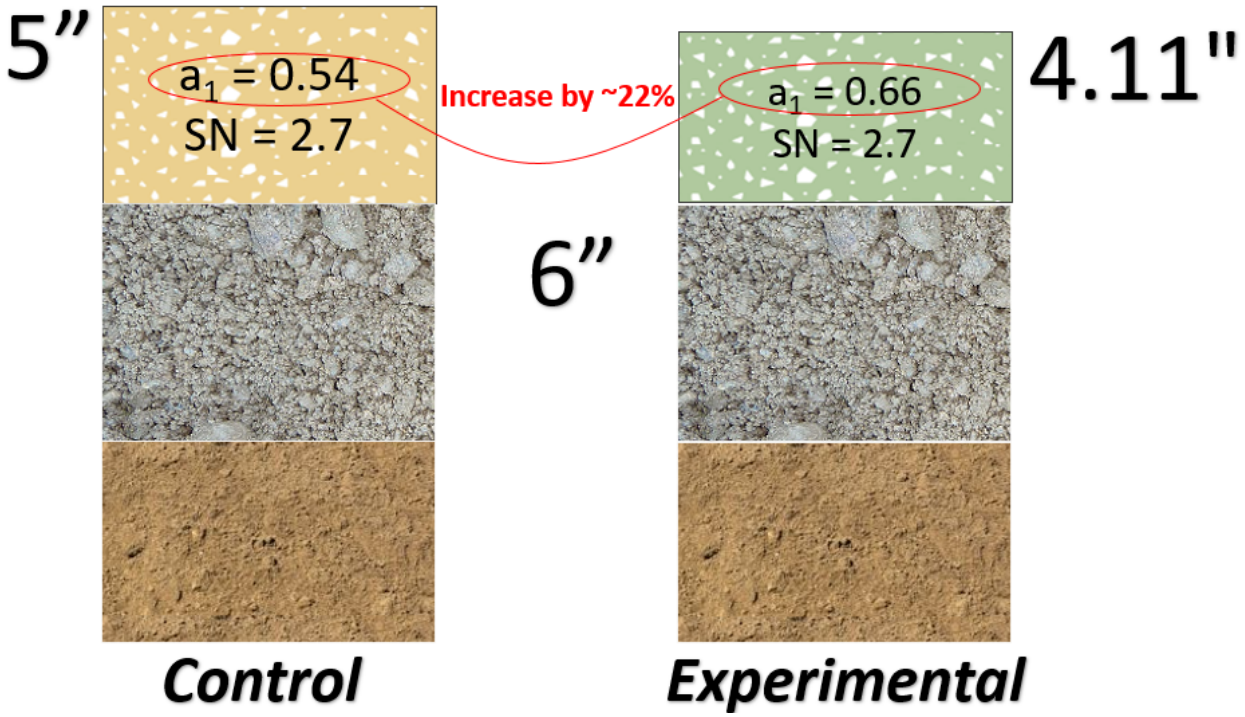

Figure 14. Structural Number Determination Based on E* at 20°C and 10 Hz.

The final structural analysis looked simply at the measured modulus values and used Equation 1 to estimate the structural coefficients as depicted in Figure 15. This analysis should not be weighed equally with that presented above because it relies on a relatively old correlation between structural coefficient and AC modulus that did not include these types of mixtures. However, it does provide a lower bound for the expected structural coefficient for each material. As shown in Figure 15, whether comparing on the basis of BBF flexural stiffness or E* at 10 Hz and 20°C, there is an increase in a_1 for the experimental mixture relative to the control. For flexural stiffness, the values are lower but indicate a 6% increase for the experimental mixture compared to the control (Table 3). The difference shrinks to 2% when comparing on the basis of E* largely due to the similarity in modulus values (Table 2). Regardless of the methodology, the determined values should be considered provisional at this point since the best measure of structural coefficient comes from calibrating to actual field performance.

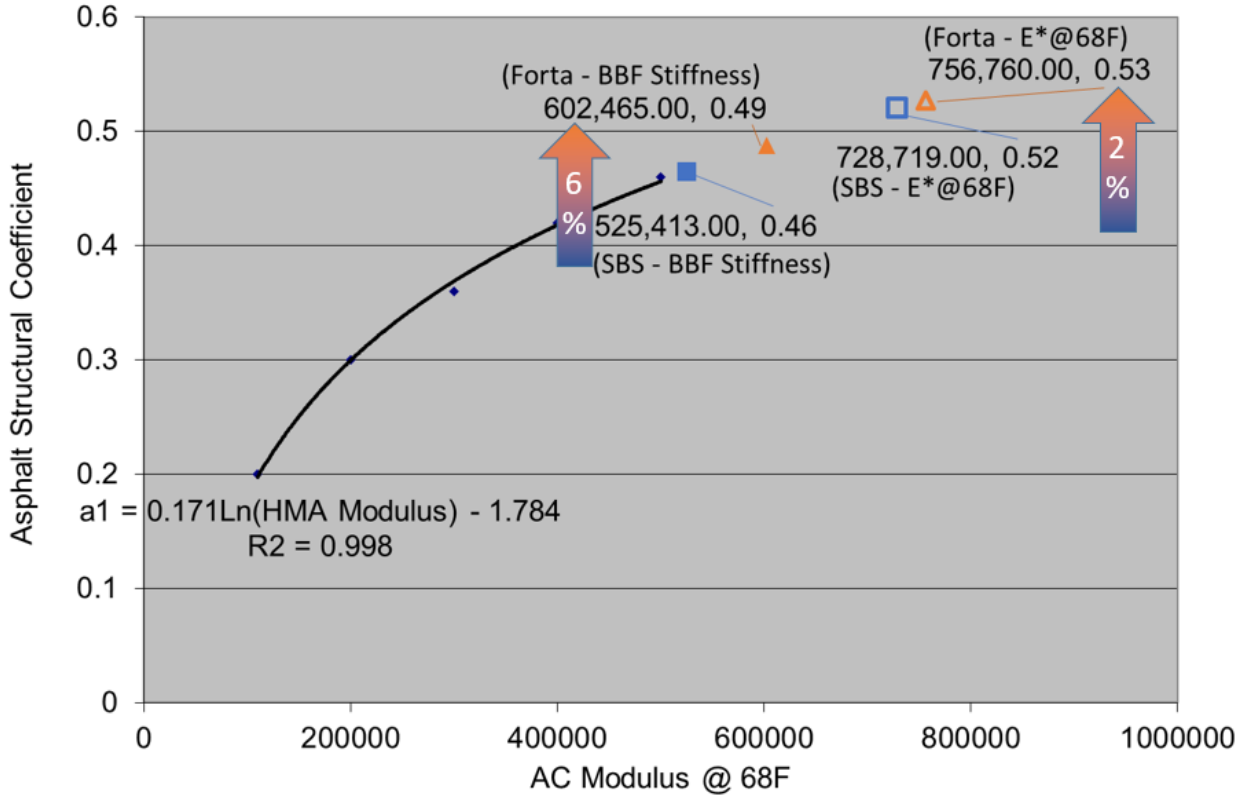

Figure 15. Structural Coefficient Estimation Based Only on Stiffness.

CONCLUSIONS

Based on the laboratory test and structural analysis results discussed above, the following conclusions can be made:

- Adding ASF slightly increased the E* of the control mixture at various combinations of test temperature and frequencies.
- Adding ASF increased the flexural stiffness but reduced the fatigue resistance of the control mixture in the BBF test when tested at intermediate and high strain levels. Compared to the control mixture, the ASF experimental mixture showed greater sensitivity of BBF N_f results to changes in strain levels. As a result, the ASF experimental mixture was expected to outperform the control mixture in terms of fatigue resistance at low strain levels.
- The structural analysis indicated, whether using flexural stiffness or E* modulus values, that the ASF mixture would have 5 to 6 times the fatigue life compared to the control mixture.
- Equivalent structures were determined which corresponded to an approximate 20% increase in structural coefficient from the control to the ASF mixture. Assigning the control mixture 0.54 resulted in an ASF structural coefficient of 0.65 or 0.66, depending on whether flexural stiffness or E* data were used in the analysis, respectively.

- Estimating structural coefficients based purely on measured modulus and correlations to structural coefficients produced smaller differences of 2 to 6% increase from the control to the ASF mixture and should be considered a lower bound.
- It is recommended that the structural coefficients determined through this analysis be considered provisional until a full-scale field evaluation may be conducted to validate the findings.

REFERENCES

Alabama Department of Transportation. Standard Specifications for Highway Construction. https://www.dot.state.al.us/conweb/pdf/Specifications/2018StandardSpecificationsCompleteBook.pdf, 2018.

American Association of State and Highway Transportation Officials. AASHTO Guide for Design of Pavement Structures. Washington D.C., 1993.